Environmental Science and Ecotechnology 22 (2024) 100458

Contents lists available at ScienceDirect

Environmental Science and Ecotechnology

journal homepage: www.journals.elsevier.com/environmental-science-and-ecotechnology/

Original Research

Seasonal dynamics of airborne biomolecules influence the size distribution of Arctic aerosols

Eunho Jang [a, b], Ki-Tae Park [a, c, *], Young Jun Yoon [a], Kyoung-Soon Jang [b, d], Min Sung Kim [b, d], Kitae Kim [a, b], Hyun Young Chung [a], Mauro Mazzola [e], David Cappelletti [e, f], Bang Yong Lee [a, b]

[a] Korea Polar Research Institute (KOPRI), Incheon, 21990, Republic of Korea
[b] University of Science and Technology (UST), Daejeon, 34113, Republic of Korea
[c] Department of Environmental Sciences and Biotechnology, Hallym University, Chuncheon, Gangwon-do, 24252, Republic of Korea
[d] Korea Basic Science Institute (KBSI), Cheongju, 28119, Republic of Korea
[e] National Research Council of Italy, Institute of Polar Sciences (CNR-ISP), Via Gobetti 101, Bologna, 40129, Italy
[f] Department of Chemistry, Biology and Biotechnology, University of Perugia, Via Elce di Sotto 8, Perugia, 06123, Italy

ARTICLE INFO

Article history:
Received 29 March 2024
Received in revised form
11 July 2024
Accepted 15 July 2024

Keywords:
Organic aerosol
FT-ICR MS
Particle size distribution
Atmospheric transport pattern
Biomolecule

ABSTRACT

Organic matter is crucial in aerosol–climate interactions, yet the physicochemical properties and origins of organic aerosols remain poorly understood. Here we show the seasonal characteristics of submicron organic aerosols in Arctic Svalbard during spring and summer, emphasizing their connection to transport patterns and particle size distribution. Microbial-derived organic matter (MOM) and terrestrial-derived organic matter (TOM) accounted for over 90% of the total organic mass in Arctic aerosols during these seasons, comprising carbohydrate/protein-like and lignin/tannin-like compounds, respectively. In spring, aerosols showed high TOM and low MOM intensities due to biomass-burning influx in the central Arctic. In contrast, summer exhibited elevated MOM intensity, attributed to the shift in predominant atmospheric transport from the central Arctic to the biologically active Greenland Sea. MOM and TOM were associated with Aitken mode particles (<100 nm diameter) and accumulation mode particles (>100 nm diameter), respectively. This association is linked to the molecular size of biomolecules, impacting the number concentrations of corresponding aerosol classes. These findings highlight the importance of considering seasonal atmospheric transport patterns and organic source-dependent particle size distributions in assessing aerosol properties in the changing Arctic.

1. Introduction

Organic aerosols (OAs) are crucial in regulating Earth's climate by influencing aerosol direct and indirect radiative forcing [1]. In the Arctic atmosphere, both anthropogenic and natural sources significantly contribute to the annual OA mass, with their relative contributions varying seasonally [2]. During the winter and early spring months (December to March), known as the Arctic haze season, OAs primarily originate from snow-covered icy areas [3], sea spray [4–6], and particles transported from distant anthropogenic sources [7]. Consequently, OAs during this period are highly oxygenated, containing significant fractions of alkane, carboxylic acid, and organosulfate functional groups [7–9]. In contrast, during summer, OAs in the Arctic atmosphere primarily stem from marine and terrestrial biogenic sources due to temperature-dependent biological activity and reduced Arctic haze effects [10,11]. This biologically productive season experiences contributions from primary and secondary aerosol sources, including biomolecules and volatile organic compounds such as dimethyl sulfide, isoprene, ammonia, and amines [12–17]. Notably, summertime OAs are characterized by a predominant fraction of hydroxyl groups [18], contributing to their high hygroscopic growth [19,20].

The aerosol size distribution in the remote Arctic exhibits pronounced seasonal variations, with primary and secondary aerosol

* Corresponding author. Department of Environmental Sciences and Biotechnology, Hallym University, Chuncheon, Gangwon-do, 24252, Republic of Korea.
E-mail address: ktp@hallym.ac.kr (K.-T. Park).

https://doi.org/10.1016/j.ese.2024.100458

Abbreviations

OAs	Organic aerosols
MOM	Microbial-derived organic matter
TOM	Terrestrial-derived organic matter
FT-ICR MS	Fourier-transform ion cyclotron resonance mass spectrometry
CHO	Compounds containing carbon, hydrogen, and oxygen
CHON	Compounds containing carbon, hydrogen, oxygen, and nitrogen
CHOS	Compounds containing carbon, hydrogen, oxygen, and sulfur
CHONS	Compounds containing carbon, hydrogen, oxygen, nitrogen, and sulfur
AI	Aromaticity index
DBE	Double bond equivalent
SMPS	Scanning mobility particle sizer
AMF	Air-mass frequency
CWT	Concentration weighted trajectory
SIC	Sea-ice concentration
PIZ	Packed ice zone
MIZ	Marginal ice zone
PAH	Polycyclic aromatic hydrocarbon

sources changing accordingly [21–24]. During winter and early spring, accumulation mode particles (>100 nm in diameter) dominate aerosol size distributions due to stable atmospheric conditions that favor the accumulation of fine aerosol precursors such as anthropogenic sulfate and black carbon [25,26]. As summer approaches, the prevalence of ultrafine particles (nucleation and Aitken mode particles; <100 nm in diameter) increases exponentially with heightened biological activity [10,27–29], accompanied by enhanced wet removal of larger particles [30,31].

The seasonal variations in aerosol chemical composition and size play a significant role in shaping the optical and hygroscopic properties of aerosols, ultimately impacting the climate system [32,33]. Despite their importance, our current understanding of seasonal variations in the molecular-level characteristics of airborne particles and their correlations with aerosol size distribution remains insufficient to fully comprehend their climate impact [34].

Analyzing specific biomarker compounds can help estimate the origin of airborne particles in pristine environments [35]. For example, multi-year studies of methanesulfonic acid have shown a strong correlation between marine biota and aerosol particles over the Arctic and Antarctic bloom periods [36–38]. Additionally, targeted analyses of polycyclic aromatic hydrocarbons and black carbon have been used to assess the contribution of fossil fuel combustion to the Arctic aerosol burden [25,39]. Recently, long-term observations of airborne levoglucosan have highlighted the warming-induced increase in biomass burning and its impact on radiative forcing in the Arctic environment [40]. However, airborne organic substances are composed of hundreds to thousands of molecules, making targeted analysis of airborne particles limited in assessing the overall chemical properties due to the complex nature of aerosol emission and transport processes [41]. Thus, a more comprehensive characterization of airborne particles using advanced analytical tools is necessary to overcome these limitations [42].

In this study, we aimed to examine the molecular-level characteristics of Arctic fine aerosols collected at Svalbard during April–August 2017. We employed non-target screening with ultrahigh-resolution 15 T Fourier-transform ion cyclotron resonance mass spectrometry (FT-ICR MS) for a detailed molecular analysis of OAs. Such non-target screening allows for profiling processes affecting the organic characteristics of airborne particles in a pristine marine environment [43,44]. Using FT-ICR MS results, we investigated the organic composition of Arctic aerosols concerning seasonal atmospheric transport patterns and their association with aerosol size distribution. Our findings could offer valuable insights into the complex nature of Arctic OAs, providing crucial information for understanding future aerosol–climate interactions.

2. Materials and methods

2.1. Aerosol measurements

We investigated the chemical properties of Arctic aerosols by analyzing fine aerosols ($PM_{2.5}$; particles with an aerodynamic equivalent diameter of <2.5 μm) collected at the rooftop of Gruvebadet Observatory, situated in Arctic Svalbard (78.5° N, 11.8° E, ~50 m above sea level; Fig. 1a), from April to August 2017. $PM_{2.5}$ particles were collected on a pre-baked quartz filter (203 × 254 mm; manufacturer-specified collection efficiency = 99.99%) using a high-volume air sampler (HV-RW, Sibata Scientific Technology, Inc.) equipped with a $PM_{2.5}$ impactor. $PM_{2.5}$ collections were performed at three-day intervals at a flow rate of 1000 L min^{-1} under ambient weather conditions, resulting in a total air volume of approximately 4320 m^3 per sample. A new round of $PM_{2.5}$ collection was initiated within an hour after the completion of the previous one, following the filter change process. A total of 52 samples were collected during the observation period. Each $PM_{2.5}$ sample was immediately stored at −20 °C to prevent chemical transformation of the collected particulate matter.

We overlapped a quarter of each sample in pairs following chronological order for molecular analysis. Organics were then extracted using 20 mL of methanol in a sonication bath for 1 h at room temperature to minimize thermal degradation of the organic matters. Sonication is commonly used to maximize the extraction efficiency for PM from filters, with extraction efficiencies for organic matter typically ranging from 60% to 90% [45,46]. Insoluble materials, such as quartz filter debris, were removed by filtering the methanolic extracts through a 0.45-μm polytetrafluoroethylene syringe filter and dried under a gentle nitrogen stream. The dried filtrates were dissolved in 50% aqueous methanol with 7% ammonium hydroxide for FT-ICR MS analysis in negative ion mode [47]. Such drying and reconstituting procedures were performed to uniformly concentrate the eluates [48,49]. The concentrated methanolic extracts were directly injected into the mass spectrometer at a flow rate of 2 μL min^{-1} using a highly precise syringe pump. We utilized a 15 T FT-ICR MS (SolariX XR™ System, Bruker Daltonics, Billerica, MA, USA), equipped with a standard electrospray ionization interface, to obtain ultrahigh-resolution mass spectra (mass-to-charge values ranging from 150 to 1000) of the extracted organics for each sample. Molecular formulas were retrieved from the dataset acquired using Bruker Compass DataAnalysis 4.2 and Sierra Analytics Composer software. Before analyzing the samples, the instrument was calibrated using an arginine solution (10 μg mL^{-1} in methanol). Molecular structures with assignment errors >0.3 ppm and those from the extract of a blank filter were excluded to minimize analytical errors.

Assigned molecular structures were categorized into four subgroups based on their elemental composition: compounds containing carbon, hydrogen, and oxygen (CHO); compounds containing carbon, hydrogen, oxygen, and nitrogen (CHON); compounds containing carbon, hydrogen, oxygen, and sulfur (CHOS);

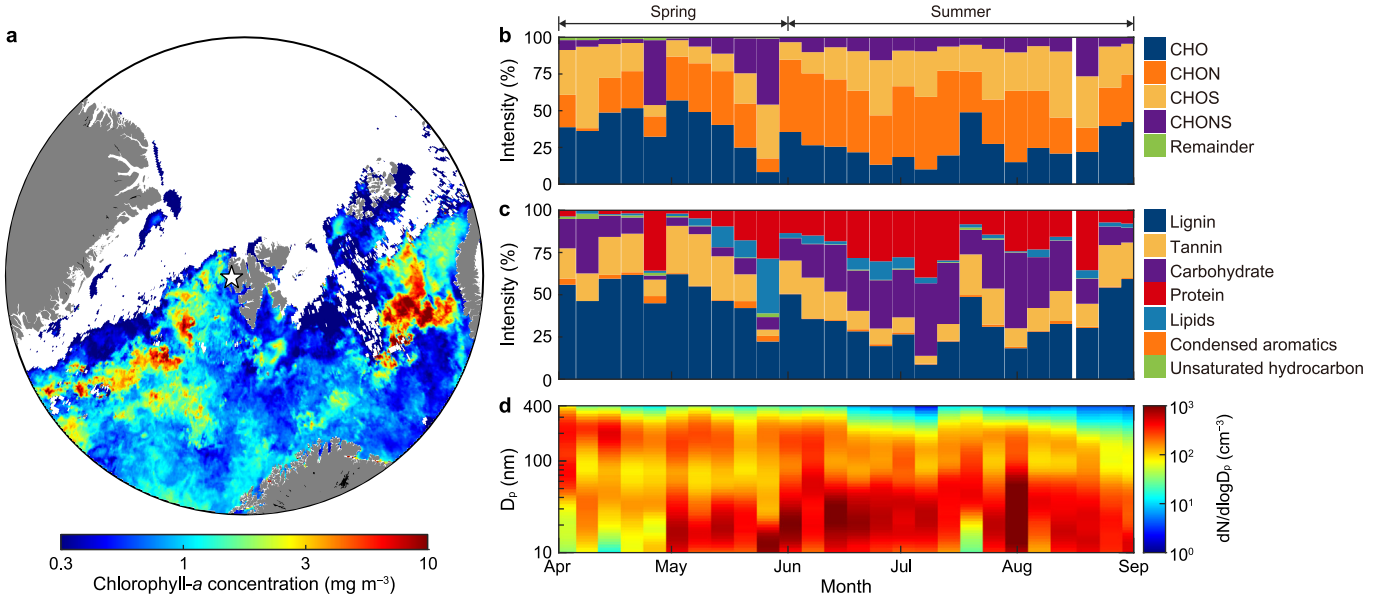

Fig. 1. a, Map indicating the location of Svalbard (white star symbol; 78.5° N, 11.8° E) and surrounding chlorophyll-*a* concentration from the MODIS-Aqua sensor in June 2017. **b**–**c,** Temporal variations in elemental (**b**) and biomolecular (**c**) compositions of Arctic aerosols derived from 15 T FT-ICR MS analysis during the observation period. **d**, aerosol size distributions within the range of 10–400 nm in diameter estimated from SMPS during the observation period. CHO: compounds containing carbon, hydrogen, and oxygen; CHON: compounds containing carbon, hydrogen, oxygen, and nitrogen; CHOS: compounds containing carbon, hydrogen, oxygen, and sulfur; CHONS; compounds containing carbon, hydrogen, oxygen, nitrogen, and sulfur.

and compounds containing carbon, hydrogen, oxygen, nitrogen, and sulfur (CHONS). Each identified molecular structure was further categorized into one of seven groups, including lignins, tannins, carbohydrates, proteins, lipids, unsaturated hydrocarbons, and condensed aromatic-like compounds, using predefined chemical metrics as illustrated in the van Krevelen diagram (Fig. 1b and c; Supplementary Material Fig. S1). In this study, the intensity of assigned molecules, indicating the signal strength of assigned molecules derived from FT-ICR MS analysis, was used to quantitatively analyze biomolecules in each $PM_{2.5}$ sample [43,50–52]. Additionally, we calculated the aromaticity index (AI) and double bond equivalent (DBE) for each biomolecule to interpret its chemical structure [53,54]. More comprehensive analytical methods for 15 T FT-ICR MS, encompassing data processing and molecular assignments, have been described in previous studies [43,47,55].

A 47-mm diameter punched disk filter was sonicated in Milli-Q water for 1 h to extract major soluble ions in the sampled aerosol. Ion chromatography (Dionex AQUION with a CS12A IonPac column for cations and Dionex ICS-1100 with an AS19 column for anions, Thermo Fisher Scientific, Inc.) was used to determine the mass concentrations of the analytes. As a tracer of biomass burning, the mass concentrations of non-sea salt potassium (nss-K^+) were calculated using the following equation: $[\text{nss-}K^+] = [K^+]_{\text{total}} - 0.037 \times [Na^+]$, where 0.037 is the mass ratio of K^+ to Na^+ in seawater [56].

Aerosol particle size distribution (within the range of 10–487 nm in mobility equivalent diameter) was measured at the Gruvebadet Observatory in Arctic Svalbard during April–August 2017, using a scanning mobility particle sizer (SMPS; TSI SMPS 3034). Each scan over the particle size range took 10 min, and we used 1-h averages in this study. As reported in previous studies, the measurement accuracy for sizing and counting with the SMPS was within ±10% [57,58]. The number concentrations of Aitken (25–100 nm diameter) and accumulation (100–400 nm diameter) mode particles were obtained from the SMPS datasets (Fig. 1d).

2.2. Trajectory outputs

Five-day air-mass back trajectories were generated using the HYbrid Single-Particle Lagrangian Integrated Trajectory (HYSPLIT) model for April–August 2017. Meteorological fields with a resolution of 0.5° × 0.5° were obtained from the global data assimilation system archive [59]. Meteorological data, such as ambient temperature, rainfall rate, and air-mass transport speed, were obtained over five-day air-mass transport pathways and averaged for each $PM_{2.5}$ sampling period. During the transition from spring to summer, both ambient temperature (from −13.8 ± 3.9 to 0.7 ± 2.5 °C) and rainfall rate (from 0.012 ± 0.008 to 0.022 ± 0.015 mm h^{-1}) increased significantly, while the seasonal difference in air-mass transport speed (from 18.1 ± 4.0 to 18.0 ± 4.7 km h^{-1}) was comparable (Supplementary Material Fig. S2). In addition, cluster analysis of the 5-day air-mass back trajectories was performed to identify major air-mass transport pathways during the observation period. The optimal number of clusters was determined based on changes in total spatial variations [59].

To identify major seasonal atmospheric transport patterns, we calculated the air-mass frequency (AMF) by summing the number of hourly endpoints in each grid cell and dividing it by the total number of hourly endpoints. Grid areas with an AMF exceeding 5% were designated as major seasonal atmospheric transport pathways. A concentration weighted trajectory (CWT) analysis was performed using the intensity of biomolecules assigned from the 15 T FT-ICR MS analysis. This analysis aimed to identify potential source regions and assess source intensity around Svalbard. CWT values in the *i*-, *j*-th grid cell ($CWT_{i,j}$) were calculated using the following equation [60]:

$$CWT_{i,j} = \frac{\sum_{k=1}^{n} C_k \tau_{i,j,k}}{\sum_{k=1}^{n} \tau_{i,j,k}}$$

where n is the total number of backward trajectories; C_k is the total

intensity of the biomolecules measured at the starting time of trajectory k; and $\tau_{i,j,k}$ is the hourly endpoint number of trajectory k in the i-, j-th grid cell.

To minimize the analytical biases in the CWT analysis for the grid cells with an extremely low number of hourly endpoints, $CWT_{i,j}$ was multiplied by an arbitrary weight function in the i-, j-th grid cell ($W_{i,j}$), as defined by Dimitriou et al. [61]. This can be expressed as follows:

$$W_{i,j} = \begin{cases} 1.0 \ (3.0n_{ave} \le n_{i,j}) \\ 0.7 \ (1.5n_{ave} \le n_{i,j} < 3.0n_{ave}) \\ 0.4 \ (n_{ave} \le n_{i,j} < 1.5n_{ave}) \\ 0.2 \ (n_{i,j} < n_{ave}) \end{cases}$$

where n_{ave} is the mean number of hourly endpoints for the entire grid cells, and $n_{i,j}$ is the number of hourly endpoints in i-, j-th grid cell. In this study, the major atmospheric transport patterns and source regions of the biomolecules were defined by the regions with the AMFs and CWT values of biomolecules above the third quartile, respectively.

2.3. Satellite-based outputs

We utilized daily sea-ice concentration (SIC) data from the National Snow and Ice Data Center to delineate geographical features in the vicinity of the Arctic Svalbard, including ocean (SIC <15%), marginal ice zone (15% ≤ SIC <80%), packed ice zone (SIC ≥80%), and land [62]. Monthly chlorophyll-*a* concentration data, obtained from the Moderate Resolution Imaging Spectroradiometer on the Aqua sensor (MODIS-Aqua), were used as a proxy for marine biological activity in the ocean surrounding the Arctic Svalbard (Fig. 1a). SIC and chlorophyll-*a* concentrations were averaged for the spring (April–May) and summer (June–August) of 2017 and regridded to a resolution of 0.5° to match the spatial resolution of the trajectory outputs.

3. Results and discussion

3.1. Seasonal characteristics of Arctic OAs

Throughout the observation period, significant variations in the chemical compositions of Arctic aerosols were observed between spring (April–May) and summer (June–August) (Fig. 1b and c). During summer, the total number and intensity of assigned molecules increased by 40% and 70%, respectively, compared to spring (Fig. 2a and b). In spring, CHO compounds were predominant, making up 39% of the total intensity. In contrast, CHON compounds became dominant during summer, contributing 39% of the total intensity (Fig. 2c).

The intensities of CHO and CHON compounds exhibited strong correlations with lignin/tannin-like compounds ($r = 0.96$, $p < 0.001$, and $n = 26$ and $r = 0.92$, $p < 0.001$, and $n = 26$, respectively) and carbohydrate/protein-like compounds ($r = 0.86$, $p < 0.001$, and $n = 26$ and $r = 0.77$, $p < 0.001$, and $n = 26$, respectively) (Supplementary Material Fig. S3). Lignin, tannin, carbohydrate, and protein-like compounds were identified as key biomolecules, contributing to more than 90% of the total assigned organic content of Arctic aerosols (Fig. 2b). Lignin/tannin-like compounds are primarily derived from terrestrial plants (terrestrial-derived organic matter, TOM), while carbohydrate/protein-like compounds are predominantly associated with microbial processes (microbial-derived organic matter, MOM) [63,64].

During summer, the intensity of MOM (i.e., levels of carbohydrate/protein-like compounds) more than doubled compared to that in spring, whereas TOM (i.e., lignin/tannin-like compounds) showed no significant seasonal variation (Fig. 2a and b). Other biomolecules, such as lipids, unsaturated hydrocarbons, and condensed aromatic-like compounds, constituted minor organic components (<10% contribution) in Arctic aerosols during both spring and summer (Fig. 2a and b). The intensities of these minor components decreased from spring to summer by 29%, 32%, and 46%, respectively (Fig. 2b).

Notably, the intensities of unsaturated hydrocarbons and condensed aromatic-like compounds were positively correlated with the intensity of the remainder group, which could not be classified into any of the four elemental classes ($r = 0.88$, $p < 0.001$, and $n = 26$ and $r = 0.63$, $p < 0.001$, and $n = 26$, respectively) (Supplementary Material Fig. S3). Previous studies conducted at the same location in 2015 suggested that this remainder group was closely associated with anthropogenic sources, such as black carbon [43]. Therefore, reducing these organics during summer may weaken localized and long-range transported anthropogenic inputs from spring to summer.

3.2. Source region-dependent biomolecular compositions of Arctic aerosols

The Svalbard Archipelago, situated in the pan-Arctic region, undergoes dynamic seasonal changes in air-mass transport patterns throughout the year [65,66]. To elucidate the source–receptor relationships of key biomolecules (i.e., TOM and MOM), we employed the AMF and CWT model based on five-day air-mass back trajectories. As depicted in Fig. 3a, significant seasonal differences were observed in the major atmospheric transport pathway (areas with AMF >5%) during spring and summer, aligning with annual climatological patterns (Supplementary Material Fig. S4). In spring, air masses primarily originated from the central Arctic, predominantly comprising the consolidated packed ice zone (PIZ) (72% PIZ, 12% marginal ice zone (MIZ), 10% ocean, and 6% land). Conversely, during summer, increased intrusion of air masses originating from the Greenland Sea led to a notable increase in advection over the ocean (45%) and MIZ (34%) compared to that during spring (Fig. 3a). This phenomenon is primarily attributed to the atmospheric pressure field around the Svalbard Archipelago, particularly the increased intrusion of southern air masses during summer. This is due to the frequent development of anticyclones around the eastern part of Svalbard, accompanied by the Icelandic low [67].

As the major atmospheric transport pathways shifted from PIZ in spring to ocean and MIZ in summer, the mean chlorophyll-*a* concentration during summer (0.58 ± 0.51 mg m^{-3}) over the major atmospheric transport pathway was over six times higher than that in spring (0.09 ± 0.29 mg m^{-3}) (Fig. 3b; Supplementary Material Fig. S5). Dissolved organic matter in the Arctic Ocean typically increases during summer due to the reduction of ice-covered areas and activation of marine biological processes [68]. This results in a significant fraction of biogenic organics in the sea surface microlayer, thereby affecting submicron aerosols in the Arctic atmosphere [11,69,70]. The observed increase in MOM contents in Arctic aerosols during summer could be attributed to rising sea spray emissions enriched with organic matter in biologically active source regions. Consequently, the summertime shift of atmospheric transport patterns into biologically active source regions could lead to a synergistic enhancement of MOM contents in the fine aerosols of the Arctic. Otherwise, along the major atmospheric transport pathways based on 5-day air-mass back trajectories, direct terrestrial organic sources were lacking during spring and summer (Fig. 3a). Consequently, external inputs of TOM could significantly influence these periods. Typically, TOM contents in Arctic aerosols peak during winter due to increased biomass-burning emissions

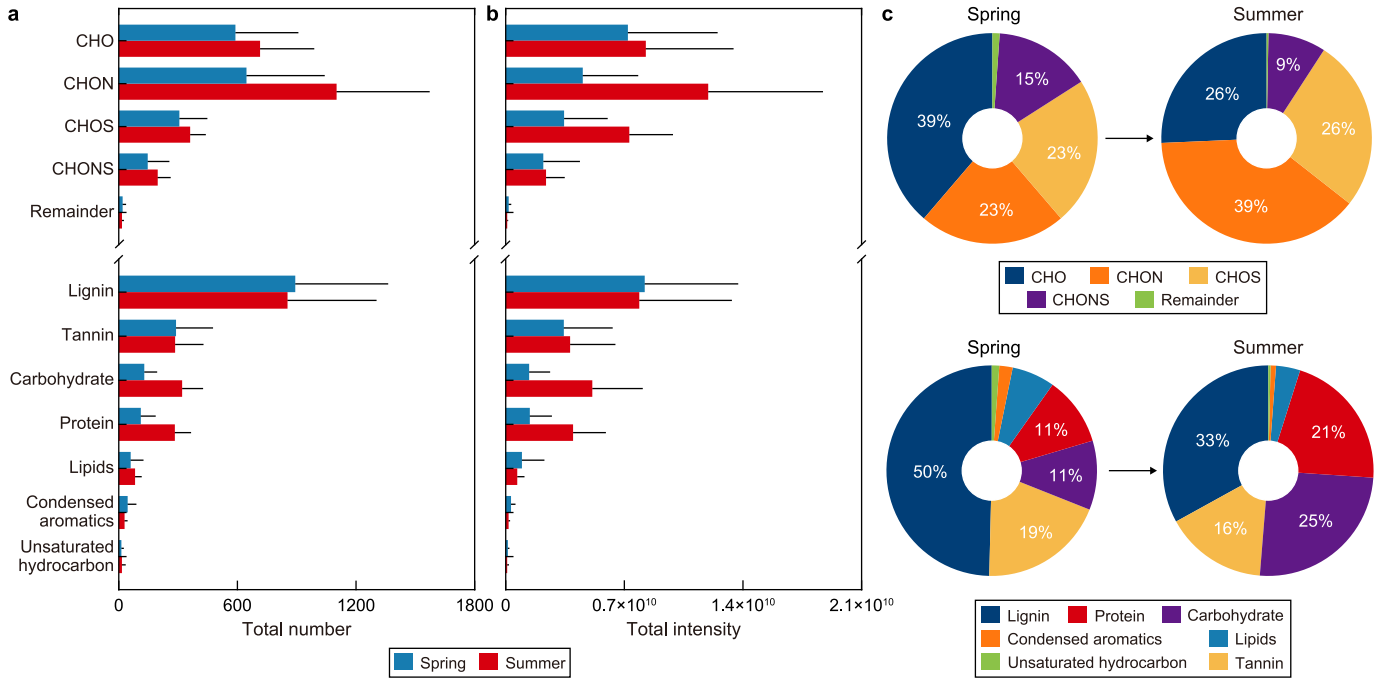

Fig. 2. **a**–**b**, The total number (**a**) and total intensity (**b**) of the Arctic aerosols during the spring and summer. **c**, The relative intensity of assigned element classes (i.e., CHO, CHON, CHOS, CHONS, and remainder) and molecular compositions (i.e., lignins, tannins, carbohydrates, proteins, lipids, condensed aromatics, and unsaturated hydrocarbon-like compounds) of the Arctic aerosols during the spring and summer. The error bar represents one standard deviation from the mean value. CHO: compounds containing carbon, hydrogen, and oxygen; CHON: compounds containing carbon, hydrogen, oxygen, and nitrogen; CHOS: compounds containing carbon, hydrogen, oxygen, and sulfur; CHONS; compounds containing carbon, hydrogen, oxygen, nitrogen, and sulfur.

[11,71,72]. These biomass-burning aerosols are readily deposited on the Arctic surface via atmospheric transport, as evidenced by high seasonal TOM and polycyclic aromatic hydrocarbon (PAH) concentrations in winter snow reported by Grannas et al. [73] and Vecchiato et al. [74], respectively. Therefore, elevated TOM levels in Arctic aerosols during spring may originate from blowing snow accumulated through snow deposition over the PIZ and from long-range transport across the central Arctic. Additionally, nss-K^+, a prominent tracer compound from biomass burning, exhibited a significant correlation with TOM intensity ($r = 0.83$, $p < 0.01$, and $n = 9$) during this period, suggesting a biomass-burning origin for springtime TOM (Supplementary Material Fig. S6a). Comparable TOM concentrations were observed in Arctic aerosols during summer (Fig. 2), coinciding with air masses originating from the ocean and MIZ (Fig. 3a). However, the tight correlation between TOM and nss-K^+ was not evident during summer ($r = 0.47$, $p = 0.10$, and $n = 14$) (Supplementary Material Fig. S6b). Previous studies indicate that soil organic matter transported via river discharge is a major contributor to Arctic Ocean organic matter during summer [43,75–78]. Hence, the lack of correlation between TOM and nss-K^+ in summer could be attributed to substantial TOM input from terrestrial sources and its subsequent release into the Arctic Ocean through river discharge. The CWT algorithm is a valuable source–receptor model for tracking the intensities of target compounds near observation sites [11,23,61]. Consistent spatial distributions of CWT values for different target compounds suggest their origin from identical source regions [61]. During the spring–summer period, the CWT values for MOM (MOM_{CWT}) and TOM (TOM_{CWT}) portrayed a positive correlation with each other ($r = 0.79$, $p < 0.001$) (Fig. 4), indicating the direct release of both organics into the Arctic atmosphere from common source regions via primary processes (e.g., bubble bursting and blowing snow).

Overall, these results imply that seasonal variations in the organic characteristics of submicron aerosols collected at Arctic Svalbard are intricately linked to changes in atmospheric transport patterns. During spring, predominant air masses originating from the central Arctic, enriched with biomass-burning sources, yield high levels of TOM but low MOM contents in Arctic OAs. Conversely, in summer, the shift of air-mass source regions toward biologically active areas, such as the ocean and MIZ, results in high MOM and TOM contents in Arctic OAs. These components originate from marine biological processes and river discharge, respectively. Such dynamics can also influence the seasonal shifts typically observed in aerosol inorganic compositions in the Arctic atmosphere, characterized by anthropogenic sources (i.e., anthropogenic-SO_4^{2-}, NO_x, inorganic halogens, and trace metals) during spring and biogenic sources (i.e., biogenic-SO_4^{2-} and NH_4^+, iodic acid) during summer [11,23]. These findings align with the conclusions of Pernov et al. [79], who suggested that changing atmospheric transport patterns significantly impact the type of aerosols in the Arctic atmosphere and highlight the significance of considering seasonal atmospheric transport patterns and associated source regions in identifying molecular characteristics of Arctic OAs.

3.3. Association of biomolecules with aerosol size distributions

Biomolecules exhibit various molecular sizes due to their diverse structures and three-dimensional conformations. Proteins and carbohydrates (i.e., MOM), composed of smaller building blocks like amino acids and monosaccharides, typically range from 1 to 100 nm in diameter [80]. This size range is attributed to their diverse physiological functions, serving as catalytic enzymes, hormones, signaling molecules, and energy sources. These multifaceted roles necessitate specific and compact chemical structures tailored to their functions [81]. In contrast, lignin and tannin (i.e.,

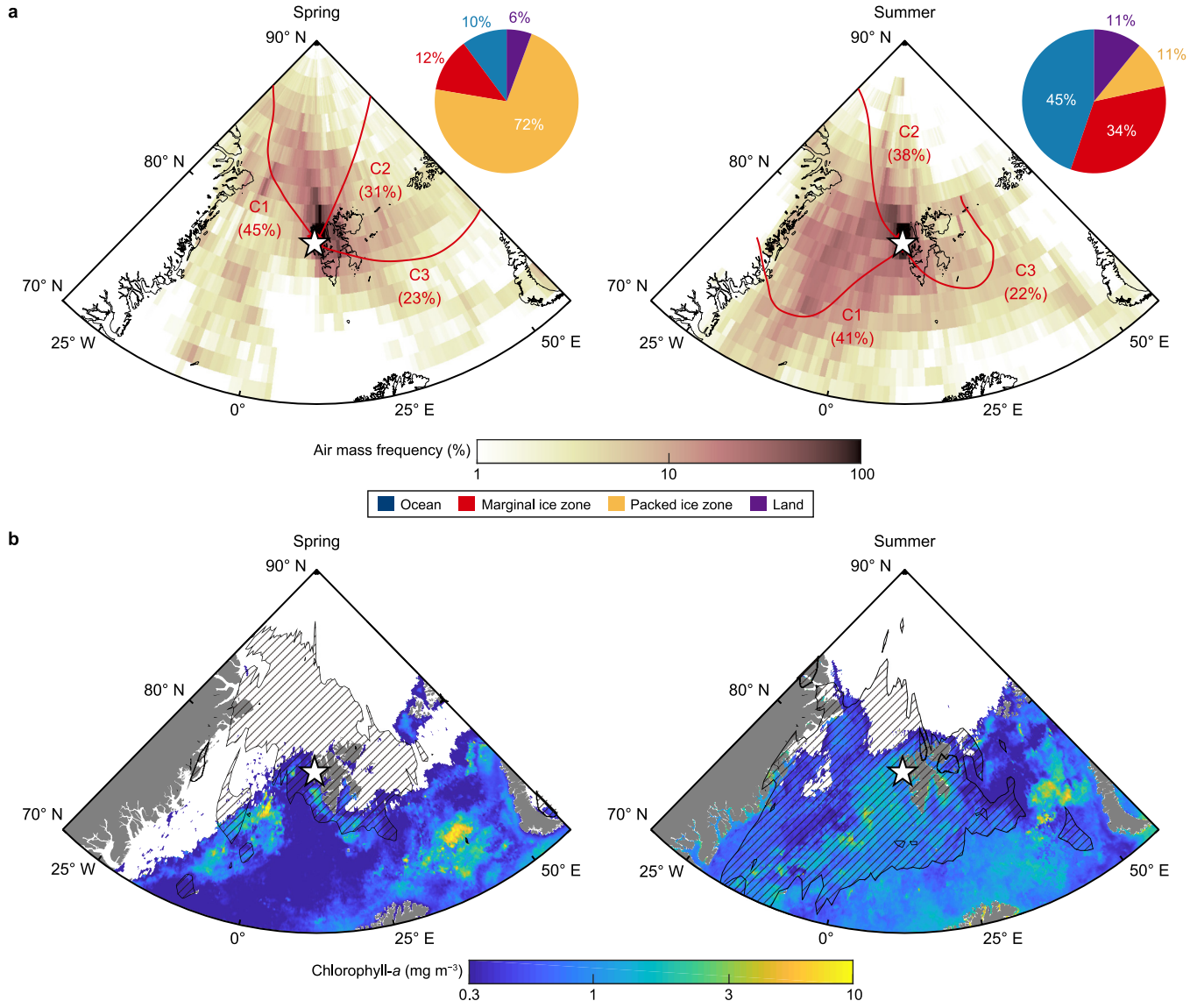

Fig. 3. **a,** Map portraying air-mass frequency (AMF) overlain with the three main clusters of the five-day air-mass back trajectory (red arrow line) during the spring and summer in 2017. Pie charts indicate geographical information, including the ocean (blue), marginal ice zone (red), packed ice zone (yellow), and land (purple), along the major atmospheric transport pathway (area with AMF >5 %). **b,** Map portraying chlorophyll-*a* concentrations during the spring and summer of 2017; the shaded area represents the areas with AMF >5 %.

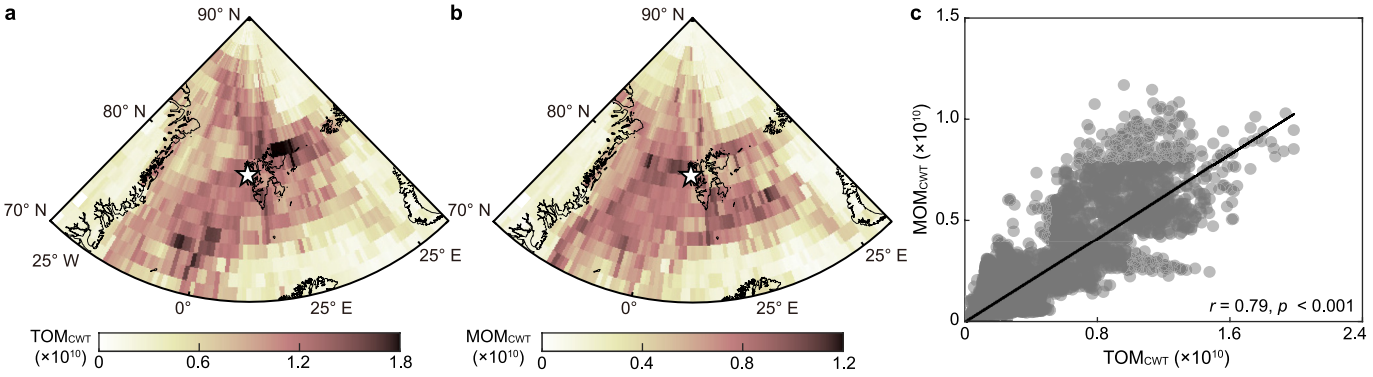

Fig. 4. **a**–**b**, Maps portraying the concentration weighted trajectory (CWT) values for the total intensity of terrestrial-derived organic matter (TOM_{CWT}; lignin and tannin, **a**) and microbial-derived organic matter (MOM_{CWT}; carbohydrate and protein, **b**) during the observation period. **c,** The relationship between the TOM_{CWT} and MOM_{CWT} during the period. The solid line indicates the best fit.

TOM), complex phenolic compounds, have larger molecular sizes exceeding 100 nm in diameter [82,83]. This is due to their highly branched and polymerized chemical structures, which provide structural support, rigidity, and protection to plant cell walls [84]. Our study observed higher values of AI (indicating the degree of aromaticity) and DBE (representing the number of double and triple bonds) for TOM (0.003–0.060 and 6.69–8.63, respectively) than those for MOM (0 and 3.2–4.0, respectively) (Supplementary Material Fig. S7). These characteristics of biomolecules may significantly influence aerosol particle size distribution.

To investigate the relationship between each biomolecule group and aerosol size distribution, we compared MOM and TOM intensities with the number concentration of Aitken (CN_{Aitken}; 25–100 nm in diameter) and accumulation (CN_{Accum}; 100–400 nm in diameter) mode particles. MOM intensity exhibited a strong correlation with Aitken mode particles ($r = 0.68$, $p < 0.01$, and $n = 26$) (Fig. 5a), underscoring the importance of microbial organics from marine biota as a crucial source of particles smaller than 100 nm. Moreover, a close correlation was observed between TOM and accumulation mode particles ($r = 0.61$, $p < 0.01$, and $n = 20$) (Fig. 5b), indicating terrestrial organics as a predominant source of larger particles. The analysis excluded periods with rainfall rates exceeding 0.03 mm h^{-1} along the air-mass transport pathway, as rainfall significantly influences aerosol size distribution via scavenging (i.e., wet deposition) (Fig. 5b). To better understand the linkage between key biomolecules and aerosol particle size distribution, we estimated the relationship between particle size-resolved number concentration in the 25–400 nm range and MOM and TOM intensities (Fig. 5c and d). Importantly, MOM exhibited a strong correlation with aerosol particles within the range of 32.3–71.8 nm in diameter (peak diameter = 54.2 nm; $r = 0.72$) (Fig. 5c). In contrast, MOM did not exhibit a statistically significant correlation with accumulation mode particles. Conversely, TOM displayed a robust correlation with smaller accumulation mode particles within the diameter range of 119.4–184.6 nm (peak diameter = 148.6 nm; $r = 0.70$), whereas no statistically significant correlation was observed with Aitken mode particles (Fig. 5d). To reinforce this discovery, we conducted a comparison between aerosol particle size distribution and the values of DBE and AI for all identified biomolecules. Notably, a robust correlation emerged between DBE values and smaller accumulation mode particles within the diameter range of 132.7–202.9 nm (peak diameter = 160.5 nm; $r = 0.69$) (Supplementary Material Fig. S8a). Considering the significant correlation observed between aerosol particle size distribution, TOM intensity, and DBE value within an overlapping particle size range (Fig. 5d; Supplementary Material Fig. S8a), it is plausible that TOM comprises a substantial number of pi-bonds and rings in its molecular structure. Consequently, this could form relatively larger aerosol particles than those associated with MOM. Furthermore, AI

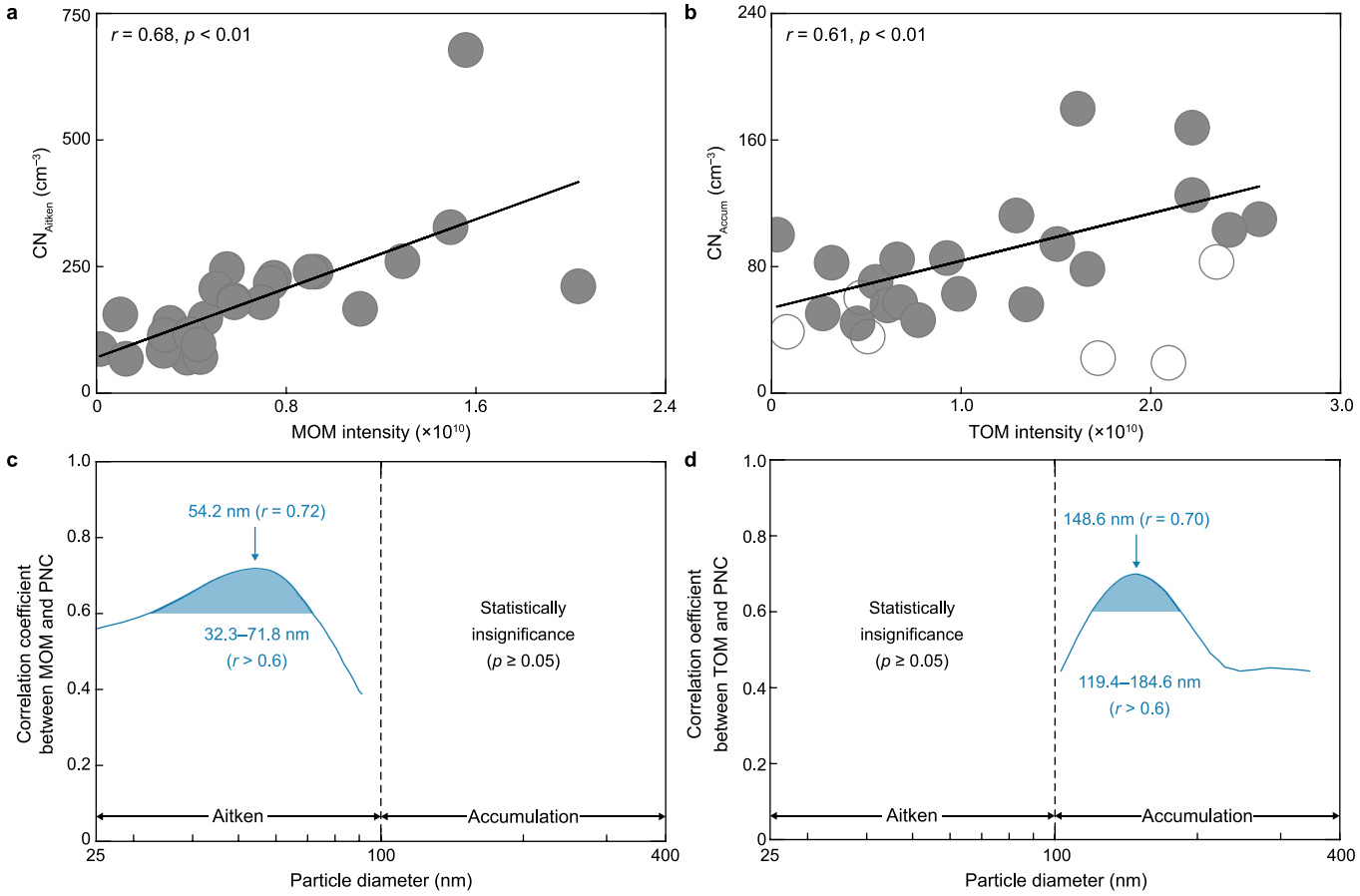

Fig. 5. a, Relationship between the total intensity of microbial-derived organic matter (MOM; carbohydrate and protein-like compounds) and number concentration of Aitken mode particles (CN_{Aitken}; 25–100 nm in diameter). **b**, Relationship between the total intensity of terrestrial-derived organic matter (TOM; lignin and tannin-like compounds) and number concentration of accumulation mode particles (CN_{Accum}; 100–400 nm in diameter). Unfilled gray circles indicate the cases with high rainfall rates >0.03 mm h^{-1} (along the air-mass transport pathway), presumably affected by wet deposition. In the regression plots, the solid lines indicate the best fit. **c–d,** The size-resolved correlation coefficients between particle number concentration (PNC) within the range of 25–400 nm with the intensity of MOM (**c**) and TOM (**d**). The shaded areas highlight the particle diameter range strongly correlated with the MOM and TOM intensities.

values demonstrated an increasing correlation with larger accumulation mode particles (Supplementary Material Fig. S8b), suggesting that biomolecules exhibiting higher AI values may be more closely associated with larger aerosol particles. However, this study did not explore the relationship between AI values and particles larger than 400 nm. These findings underscore the distinct influence of molecular structure-dependent sizes of MOM and TOM on aerosol size distribution, with MOM predominantly associated with Aitken mode particles and TOM with accumulation mode particles. Consequently, during summer, the number concentration of Aitken mode particles was two-fold greater than during spring, whereas the difference in the accumulation mode particle concentration was comparable, reflecting a parallel seasonal trend observed for TOM and MOM (Supplementary Material Fig. S9).

In the pristine Arctic atmosphere, Aitken mode particles constitute a significant portion of particle number concentration and play a critical role in cloud condensation nuclei activation, thereby influencing radiative forcing [14,32,85,86]. The dominant source of Aitken mode particles in the Arctic atmosphere is the formation of new particles with diameters <10 nm via gas-to-particle conversion [29,68,87,88]. The robust correlation between MOM and particles <100 nm suggests that protein and carbohydrate compounds produced via marine biogenic primary sources may significantly influence the formation of climate-relevant Aitken mode particles. This influence is evident in their ability to elucidate ~50% of the variance in the number concentration of Aitken mode particles during spring to summer (Fig. 5a), coinciding with drastic changes in atmospheric transport patterns and biological activity affecting aerosol physiochemical properties. These findings underscore the significance of seasonal characteristics of Arctic OAs in understanding aerosol size distribution in the region.

4. Conclusions

With the ongoing Arctic warming [89], the counteracting effects of biogenic OAs have garnered significant attention in recent decades. Numerous studies have endeavored to elucidate the potential anthropogenic and biogenic organic sources, their seasonal transitions, and their impact on the chemical properties of Arctic OAs [9,11,69,90,91]. Recently, a limited number of field observations have delved into the molecular composition of aerosol particles in the Arctic and Antarctic atmosphere utilizing high-resolution mass spectrometry. These investigations have unveiled hundreds to thousands of individual aerosol constituents in pristine marine environments [43,44]. However, studies examining aerosol–climate interactions, particularly those analyzing the biomolecular characteristics of Arctic OAs and their correlations with aerosol size distribution, are limited. In this study, we demonstrate that the molecular characteristics of biomolecules, depending on their origin, are directly linked to the size distribution of aerosol particles. Specifically, MOM and TOM closely connect with Aitken and accumulation mode particles, respectively. Furthermore, our findings emphasize the significant impact of seasonal atmospheric transport patterns on the biomolecular composition of Arctic OAs. These findings were facilitated by combining seasonal variations of non-target screening molecular complex analysis results with size number distribution datasets and various satellite estimates.

In recent decades, warming-induced sea-ice decline has precipitated substantial concurrent changes in both marine and terrestrial ecosystems, including drastic decadal increases in biological activity in the Arctic Ocean and the greening of the Arctic tundra [92–95]. Collectively, the ongoing increase in riverine input and wind-wave extremes in the Arctic Ocean [96,97], along with the frequent intrusion of warm and moist air masses from Eastern Europe into the Arctic Ocean [98,99], potentially contribute to the augmentation of atmospheric MOM and TOM levels, thereby significantly impacting the abundance of Arctic aerosols measuring tens to hundreds of nanometers in diameter. Therefore, it is crucial to understand future changes in atmospheric transport patterns and the source region-dependent compositions and intensities of OA precursors to accurately assess future aerosol–climate interactions in the Arctic atmosphere. However, this study did not address the influence of secondary aerosol formation processes and the effects of chemical transformations on aerosol size distribution owing to limited field measurements of atmospheric aerosol precursors such as sulfuric and iodic acids, ammonia, and amines. For a more comprehensive understanding of aerosol–climate interactions in the Arctic, unified monitoring of the physicochemical properties of aerosols and various precursor compounds must be conducted in areas vulnerable to climate change.

CRediT authorship contribution statement

Eunho Jang: Writing - Review & Editing, Writing - Original Draft, Visualization, Formal analysis. **Ki-Tae Park:** Writing - Review & Editing, Writing - Original Draft, Supervision, Conceptualization. **Young Jun Yoon:** Writing - Review & Editing, Conceptualization. **Kyoung-Soon Jang:** Writing - Review & Editing, Conceptualization. **Min Sung Kim:** Writing - Review & Editing, Investigation. **Kitae Kim:** Writing - Review & Editing, Conceptualization. **Hyun Young Chung:** Writing - Review & Editing, Investigation. **Mauro Mazzola:** Writing - Review & Editing, Investigation. **David Cappelletti:** Writing - Review & Editing. **Bang Yong Lee:** Writing - Review & Editing, Resources.

Declaration of competing interest

The authors declare that they have no known competing financial interests or personal relationships that could have appeared to influence the work reported in this paper.

Acknowledgements

This work was supported by the National Research Foundation (NRF) of Korea NRF-2021M1A5A1065425 (KOPRI-PN24011). The FT-ICR MS analysis was supported by the Korea Basic Science Institute under the R&D program (Project No. C330430) supervised by the Ministry of Science and ICT. We would like to extend our gratitude to our Italian colleagues at the Italian National Council of Research (CNR) for hosting our aerosol sampler at the Gruvebadet Observatory.

Appendix A. Supplementary data

Supplementary data to this article can be found online at https://doi.org/10.1016/j.ese.2024.100458.

References

[1] E.K. Bigg, C. Leck, Cloud-active particles over the central Arctic Ocean, J. Geophys. Res. Atmos. 106 (D23) (2001) 32155–32166, https://doi.org/10.1029/1999JD901152.
[2] R. Lange, M. Dall'Osto, H. Wex, H. Skov, A. Massling, Large summer contribution of organic biogenic aerosols to arctic cloud condensation nuclei, Geophys. Res. Lett. 46 (20) (2019) 11500–11509, https://doi.org/10.1029/2019GL084142.
[3] X. Gong, J. Zhang, B. Croft, X. Yang, M.M. Frey, N. Bergner, R.Y.W. Chang, J.M. Creamean, C. Kuang, R.V. Martin, A. Ranjithkumar, A.J. Sedlacek, J. Uin, S. Willmes, M.A. Zawadowicz, J.R. Pierce, M.D. Shupe, J. Schmale, J. Wang, Arctic warming by abundant fine sea salt aerosols from blowing snow, Nat. Geosci. 16 (9) (2023) 768–774, https://doi.org/10.1038/s41561-023-01254-8.
[4] K. Hara, S. Matoba, M. Hirabayashi, T. Yamasaki, Frost flowers and sea-salt aerosols over seasonal sea-ice areas in northwestern Greenland during

winter–spring, Atmos. Chem. Phys. 17 (13) (2017) 8577–8598, https://doi.org/10.5194/acp-17-8577-2017.
[5] J. Huang, L. Jaeglé, Wintertime enhancements of sea salt aerosol in polar regions consistent with a sea ice source from blowing snow, Atmos. Chem. Phys. 17 (5) (2017) 3699–3712, https://doi.org/10.5194/acp-17-3699-2017.
[6] E. Ioannidis, K.S. Law, J.C. Raut, L. Marelle, T. Onishi, R.M. Kirpes, L.M. Upchurch, T. Tuch, A. Wiedensohler, A. Massling, H. Skov, P.K. Quinn, K.A. Pratt, Modelling wintertime sea-spray aerosols under Arctic haze conditions, Atmos. Chem. Phys. 23 (10) (2023) 5641–5678, https://doi.org/10.5194/acp-23-5641-2023.
[7] A.A. Frossard, P.M. Shaw, L.M. Russell, J.H. Kroll, M.R. Canagaratna, D.R. Worsnop, P.K. Quinn, T.S. Bates, Springtime Arctic haze contributions of submicron organic particles from European and Asian combustion sources, J. Geophys. Res. Atmos. 116 (D5) (2011), https://doi.org/10.1029/2010JD015178.
[8] R.M. Kirpes, A.L. Bondy, D. Bonanno, R.C. Moffet, B. Wang, A. Laskin, A.P. Ault, K.A. Pratt, Secondary sulfate is internally mixed with sea spray aerosol and organic aerosol in the winter Arctic, Atmos. Chem. Phys. 18 (6) (2018) 3937–3949, https://doi.org/10.5194/acp-18-3937-2018.
[9] P.M. Shaw, L.M. Russell, A. Jefferson, P.K. Quinn, Arctic organic aerosol measurements show particles from mixed combustion in spring haze and from frost flowers in winter, Geophys. Res. Lett. 37 (10) (2010), https://doi.org/10.1029/2010GL042831.
[10] B. Croft, R.V. Martin, W.R. Leaitch, J. Burkart, R.Y.W. Chang, D.B. Collins, P.L. Hayes, A.L. Hodshire, L. Huang, J.K. Kodros, A. Moravek, E.L. Mungall, J.G. Murphy, S. Sharma, S. Tremblay, G.R. Wentworth, M.D. Willis, J.P.D. Abbatt, J.R. Pierce, Arctic marine secondary organic aerosol contributes significantly to summertime particle size distributions in the Canadian Arctic Archipelago, Atmos. Chem. Phys. 19 (5) (2019) 2787–2812, https://doi.org/10.5194/acp-19-2787-2019.
[11] V. Moschos, K. Dzepina, D. Bhattu, H. Lamkaddam, R. Casotto, K.R. Daellenbach, F. Canonaco, P. Rai, W. Aas, S. Becagli, G. Calzolai, K. Eleftheriadis, C.E. Moffett, J. Schnelle-Kreis, M. Severi, S. Sharma, H. Skov, M. Vestenius, W. Zhang, I. El Haddad, Equal abundance of summertime natural and wintertime anthropogenic Arctic organic aerosols, Nat. Geosci. 15 (3) (2022) 196–202, https://doi.org/10.1038/s41561-021-00891-1.
[12] J.D. Allan, W.T. Morgan, E. Darbyshire, M.J. Flynn, P.I. Williams, D.E. Oram, P. Artaxo, J. Brito, J.D. Lee, H. Coe, Airborne observations of IEPOX-derived isoprene SOA in the Amazon during SAMBBA, Atmos. Chem. Phys. 14 (20) (2014) 11393–11407, https://doi.org/10.5194/acp-14-11393-2014.
[13] A. Baccarini, L. Karlsson, J. Dommen, P. Duplessis, J. Vüllers, I.M. Brooks, A. Saiz-Lopez, M. Salter, M. Tjernström, U. Baltensperger, P. Zieger, J. Schmale, Frequent new particle formation over the high Arctic pack ice by enhanced iodine emissions, Nat. Commun. 11 (1) (2020) 4924, https://doi.org/10.1038/s41467-020-18551-0.
[14] B. Croft, G.R. Wentworth, R.V. Martin, W.R. Leaitch, J.G. Murphy, B.N. Murphy, J.K. Kodros, J.P.D. Abbatt, J.R. Pierce, Contribution of Arctic seabird-colony ammonia to atmospheric particles and cloud-albedo radiative effect, Nat. Commun. 7 (1) (2016) 13444, https://doi.org/10.1038/ncomms13444.
[15] M. Feltracco, E. Barbaro, T. Kirchgeorg, A. Spolaor, C. Turetta, R. Zangrando, C. Barbante, A. Gambaro, Free and combined L- and D-amino acids in Arctic aerosol, Chemosphere 220 (2019) 412–421, https://doi.org/10.1016/j.chemosphere.2018.12.147.
[16] R. Ghahreman, W. Gong, M. Galí, A.L. Norman, S.R. Beagley, A. Akingunola, Q. Zheng, A. Lupu, M. Lizotte, M. Levasseur, W.R. Leaitch, Dimethyl sulfide and its role in aerosol formation and growth in the Arctic summer – a modelling study, Atmos. Chem. Phys. 19 (23) (2019) 14455–14476, https://doi.org/10.5194/acp-19-14455-2019.
[17] G.R. Wentworth, J.G. Murphy, B. Croft, R.V. Martin, J.R. Pierce, J.S. Côté, I. Courchesne, J.É. Tremblay, J. Gagnon, J.L. Thomas, S. Sharma, D. Toom-Sauntry, A. Chivulescu, M. Levasseur, J.P.D. Abbatt, Ammonia in the summertime Arctic marine boundary layer: sources, sinks, and implications, Atmos. Chem. Phys. 16 (4) (2016) 1937–1953, https://doi.org/10.5194/acp-16-1937-2016.
[18] J. Liu, J. Dedrick, L.M. Russell, G.I. Senum, J. Uin, C. Kuang, S.R. Springston, W.R. Leaitch, A.C. Aiken, D. Lubin, High summertime aerosol organic functional group concentrations from marine and seabird sources at Ross Island, Antarctica, during AWARE, Atmos. Chem. Phys. 18 (12) (2018) 8571–8587, https://doi.org/10.5194/acp-18-8571-2018.
[19] K.A. Malek, K. Gohil, H.A. Al-Abadleh, A.A. Asa-Awuku, Hygroscopicity of polycatechol and polyguaiacol secondary organic aerosol in sub- and supersaturated water vapor environments, Environ. Sci.: Atmos. 2 (1) (2022) 24–33, https://doi.org/10.1039/D1EA00063B.
[20] A. Massling, R. Lange, J.B. Pernov, U. Gosewinkel, L.L. Sørensen, H. Skov, Measurement report: high Arctic aerosol hygroscopicity at sub- and supersaturated conditions during spring and summer, Atmos. Chem. Phys. 23 (8) (2023) 4931–4953, https://doi.org/10.5194/acp-23-4931-2023.
[21] M. Dall'Osto, D.C.S. Beddows, P. Tunved, R.M. Harrison, A. Lupi, V. Vitale, S. Becagli, R. Traversi, K.T. Park, Y.J. Yoon, A. Massling, H. Skov, R. Lange, J. Strom, R. Krejci, Simultaneous measurements of aerosol size distributions at three sites in the European high Arctic, Atmos. Chem. Phys. 19 (11) (2019) 7377–7395, https://doi.org/10.5194/acp-19-7377-2019.
[22] E. Freud, R. Krejci, P. Tunved, R. Leaitch, Q.T. Nguyen, A. Massling, H. Skov, L. Barrie, Pan-Arctic aerosol number size distributions: seasonality and transport patterns, Atmos. Chem. Phys. 17 (13) (2017) 8101–8128, https://doi.org/10.5194/acp-17-8101-2017.
[23] C. Song, S. Becagli, D.C.S. Beddows, J. Brean, J. Browse, Q. Dai, M. Dall'Osto, V. Ferracci, R.M. Harrison, N. Harris, W. Li, A.E. Jones, A. Kirchgäßner, A.G. Kramawijaya, A. Kurganskiy, A. Lupi, M. Mazzola, M. Severi, R. Traversi, Z. Shi, Understanding sources and drivers of size-resolved aerosol in the high Arctic Islands of Svalbard using a receptor model coupled with machine learning, Environ. Sci. Technol. 56 (16) (2022) 11189–11198, https://doi.org/10.1021/acs.est.1c07796.
[24] P. Tunved, J. Ström, R. Krejci, Arctic aerosol life cycle: linking aerosol size distributions observed between 2000 and 2010 with air mass transport and precipitation at Zeppelin station, Ny-Ålesund, Svalbard, Atmos. Chem. Phys. 13 (7) (2013) 3643–3660, https://doi.org/10.5194/acp-13-3643-2013.
[25] L. Ren, Y. Yang, H. Wang, R. Zhang, P. Wang, H. Liao, Source attribution of Arctic black carbon and sulfate aerosols and associated Arctic surface warming during 1980–2018, Atmos. Chem. Phys. 20 (14) (2020) 9067–9085, https://doi.org/10.5194/acp-20-9067-2020.
[26] Y. Yang, H. Wang, S.J. Smith, R.C. Easter, P.J. Rasch, Sulfate aerosol in the Arctic: source attribution and radiative forcing, J. Geophys. Res. Atmos. 123 (3) (2018) 1899–1918, https://doi.org/10.1002/2017JD027298.
[27] J. Heintzenberg, C. Leck, P. Tunved, Potential source regions and processes of aerosol in the summer Arctic, Atmos. Chem. Phys. 15 (11) (2015) 6487–6502, https://doi.org/10.5194/acp-15-6487-2015.
[28] M.J. Lawler, E.S. Saltzman, L. Karlsson, P. Zieger, M. Salter, A. Baccarini, J. Schmale, C. Leck, New insights into the composition and origins of ultrafine aerosol in the summertime high Arctic, Geophys. Res. Lett. 48 (21) (2021) e2021GL094395, https://doi.org/10.1029/2021GL094395.
[29] K.-T. Park, S. Jang, K. Lee, Y.J. Yoon, M.S. Kim, K. Park, H.J. Cho, J.H. Kang, R. Udisti, B.Y. Lee, K.H. Shin, Observational evidence for the formation of DMS-derived aerosols during Arctic phytoplankton blooms, Atmos. Chem. Phys. 17 (15) (2017) 9665–9675, https://doi.org/10.5194/acp-17-9665-2017.
[30] T. Garrett, C. Zhao, P. Novelli, Assessing the relative contributions of transport efficiency and scavenging to seasonal variability in Arctic aerosol, Tellus B 62 (3) (2010) 190–196, https://doi.org/10.1111/j.1600-0889.2010.00453.x.
[31] M.D. Willis, W.R. Leaitch, J.P.D. Abbatt, Processes controlling the composition and abundance of Arctic aerosol, Rev. Geophys. 56 (4) (2018) 621–671, https://doi.org/10.1029/2018RG000602.
[32] I. Bulatovic, A.L. Igel, C. Leck, J. Heintzenberg, I. Riipinen, A.M.L. Ekman, The importance of Aitken mode aerosol particles for cloud sustenance in the summertime high Arctic – a simulation study supported by observational data, Atmos. Chem. Phys. 21 (5) (2021) 3871–3897, https://doi.org/10.5194/acp-21-3871-2021.
[33] L. Schmeisser, E. Andrews, J.A. Ogren, P. Sheridan, A. Jefferson, S. Sharma, J.E. Kim, J.P. Sherman, M. Sorribas, I. Kalapov, T. Arsov, C. Angelov, O.L. Mayol-Bracero, C. Labuschagne, S.W. Kim, A. Hoffer, N.H. Lin, H.P. Chia, M. Bergin, H. Wu, Classifying aerosol type using in situ surface spectral aerosol optical properties, Atmos. Chem. Phys. 17 (19) (2017) 12097–12120, https://doi.org/10.5194/acp-17-12097-2017.
[34] J. Schmale, P. Zieger, A.M.L. Ekman, Aerosols in current and future Arctic climate, Nat. Clim. Change 11 (2) (2021) 95–105, https://doi.org/10.1038/s41558-020-00969-5.
[35] B.R.T. Simoneit, A review of biomarker compounds as source indicators and tracers for air pollution, Environ. Sci. Pollut. Res. 6 (3) (1999) 159–169, https://doi.org/10.1007/BF02987621.
[36] S. Becagli, E. Barbaro, S. Bonamano, L. Caiazzo, A. di Sarra, M. Feltracco, P. Grigioni, J. Heintzenberg, L. Lazzara, M. Legrand, A. Madonia, M. Marcelli, C. Melillo, D. Meloni, C. Nuccio, G. Pace, K.T. Park, S. Preunkert, M. Severi, R. Traversi, Factors controlling atmospheric DMS and its oxidation products (MSA and $nssSO_4^{2-}$) in the aerosol at Terra Nova Bay, Antarctica, Atmos. Chem. Phys. 22 (14) (2022) 9245–9263, https://doi.org/10.5194/acp-22-9245-2022.
[37] S.-B. Hong, Y.J. Yoon, S. Becagli, Y. Gim, S.D. Chambers, K.-T. Park, S.-J. Park, R. Traversi, M. Severi, V. Vitale, J.-H. Kim, E. Jang, J. Crawford, A.D. Griffiths, Seasonality of aerosol chemical composition at king Sejong station (Antarctic Peninsula) in 2013, Atmos. Environ. 223 (2020) 117185, https://doi.org/10.1016/j.atmosenv.2019.117185.
[38] S. Jang, K.T. Park, K. Lee, Y.J. Yoon, K. Kim, H.Y. Chung, E. Jang, S. Becagli, B.Y. Lee, R. Traversi, K. Eleftheriadis, R. Krejci, O. Hermansen, Large seasonal and interannual variations of biogenic sulfur compounds in the Arctic atmosphere (Svalbard; 78.9°N, 11.9°E), Atmos. Chem. Phys. 21 (12) (2021) 9761–9777, https://doi.org/10.5194/acp-21-9761-2021.
[39] Y. Yu, A. Katsoyiannis, P. Bohlin-Nizzetto, E. Brorström-Lundén, J. Ma, Y. Zhao, Z. Wu, W. Tych, D. Mindham, E. Sverko, E. Barresi, H. Dryfhout-Clark, P. Fellin, H. Hung, Polycyclic aromatic hydrocarbons not declining in Arctic air despite global emission reduction, Environ. Sci. Technol. 53 (5) (2019) 2375–2382, https://doi.org/10.1021/acs.est.8b05353.
[40] A. Chen, Z. Xie, H. Zhan, B. Jiang, A. Zhang, H. Liu, C. Hu, X. Wu, F. Yue, L. Xu, Long-term observations of levoglucosan in arctic aerosols reveal its biomass burning source and implication on radiative forcing, J. Geophys. Res. Atmos. 128 (12) (2023) e2022JD037597, https://doi.org/10.1029/2022JD037597.
[41] B. Gantt, N. Meskhidze, The physical and chemical characteristics of marine primary organic aerosol: a review, Atmos. Chem. Phys. 13 (2013) 3979–3996, https://doi.org/10.5194/acp-13-3979-2013.
[42] S.D. Brooks, D.C.O. Thornton, Marine aerosols and clouds, Ann. Rev. Mar. Sci 10 (1) (2018) 289–313, https://doi.org/10.1146/annurev-marine-121916-063148.

[43] J.H. Choi, E. Jang, Y.J. Yoon, J.Y. Park, T.-W. Kim, S. Becagli, L. Caiazzo, D. Cappelletti, R. Krejci, K. Eleftheriadis, K.-T. Park, K.S. Jang, Influence of biogenic organics on the chemical composition of arctic aerosols, Glob. Biogeochem. Cy. 33 (10) (2019) 1238–1250, https://doi.org/10.1029/2019GB006226.
[44] J. Jang, K.-T. Park, Y.J. Yoon, S.-Y. Ha, E. Jang, K.H. Cho, J.Y. Lee, J. Park, Molecular-level chemical composition of aerosol and its potential source tracking at Antarctic Peninsula, Environ. Res. 239 (2023) 117217, https://doi.org/10.1016/j.envres.2023.117217.
[45] R. Devlin, Standard Operating Procedure for Extraction of Concentrated Particulate Matter from PUF and G5300 Media. National Health and Environmental Effects Research Laboratory, U.S. Environmental Protection Agency, Personal communication, Research Triangle Park, NC, 2009.
[46] C. Roper, L.G. Chubb, L. Cambal, B. Tunno, J.E. Clougherty, S.E. Mischler, Characterization of ambient and extracted PM2.5 collected on filters for toxicology applications, Inhal. Toxicol. 27 (13) (2015) 673–681, https://doi.org/10.3109/08958378.2015.1092185.
[47] J.H. Choi, Y.-G. Kim, Y.K. Lee, S.P. Pack, J.Y. Jung, K.-S. Jang, Chemical characterization of dissolved organic matter in moist acidic tussock tundra soil using ultra-high resolution 15T FT-ICR mass spectrometry, Biotechnol. Bioproc. Eng. 22 (5) (2017) 637–646, https://doi.org/10.1007/s12257-017-0121-4.
[48] P. Lin, A.G. Rincon, M. Kalberer, J.Z. Yu, Elemental composition of HULIS in the Pearl river Delta region, China: results Inferred from positive and negative electrospray high resolution mass spectrometric data, Environ. Sci. Technol. 46 (14) (2012) 7454–7462, https://doi.org/10.1021/es300285d.
[49] P. Lin, J.Z. Yu, G. Engling, M. Kalberer, Organosulfates in Humic-like substance fraction isolated from aerosols at seven locations in East Asia: a study by ultra-high-resolution mass spectrometry, Environ. Sci. Technol. 46 (24) (2012) 13118–13127, https://doi.org/10.1021/es303570v.
[50] M. Cui, C. Li, Y. Chen, F. Zhang, J. Li, B. Jiang, Y. Mo, J. Li, C. Yan, M. Zheng, Z. Xie, G. Zhang, J. Zheng, Molecular characterization of polar organic aerosol constituents in off-road engine emissions using Fourier transform ion cyclotron resonance mass spectrometry (FT-ICR MS): implications for source apportionment, Atmos. Chem. Phys. 19 (22) (2019) 13945–13956, https://doi.org/10.5194/acp-19-13945-2019.
[51] C. Ning, Y. Gao, H. Yu, H. Zhang, N. Geng, R. Cao, J. Chen, FT-ICR mass spectrometry for molecular characterization of water-insoluble organic compounds in winter atmospheric fine particulate matters, J. Environ. Sci. 111 (2022) 51–60, https://doi.org/10.1016/j.jes.2020.12.017.
[52] E. Schneider, H. Czech, O. Popovicheva, M. Chichaeva, V. Kobelev, N. Kasimov, T. Minkina, C.P. Rüger, R. Zimmermann, Mass spectrometric analysis of unprecedented high levels of carbonaceous aerosol particles long-range transported from wildfires in the Siberian Arctic, Atmos. Chem. Phys. 24 (1) (2024) 553–576, https://doi.org/10.5194/acp-24-553–2024.
[53] A. Stubbins, R.G.M. Spencer, H. Chen, P.G. Hatcher, K. Mopper, P.J. Hernes, V.L. Mwamba, A.M. Mangangu, J.N. Wabakanghanzi, J. Six, Illuminated darkness: molecular signatures of Congo River dissolved organic matter and its photochemical alteration as revealed by ultrahigh precision mass spectrometry, Limnol. Oceanogr. 55 (4) (2010) 1467–1477, https://doi.org/10.4319/lo.2010.55.4.1467.
[54] B.P. Koch, T. Dittmar, From mass to structure: an aromaticity index for high-resolution mass data of natural organic matter, Rapid Commun. Mass Spectrom. 20 (5) (2006) 926–932, https://doi.org/10.1002/rcm.2386.
[55] M. Choi, A.Y. Choi, S.-Y. Ahn, K.-Y. Choi, K.-S. Jang, Characterization of molecular composition of bacterial melanin isolated from *Streptomyces glaucescens* using ultra-high-resolution FT-ICR mass spectrometry, Mass Spectrom. Lett. 9 (3) (2018) 81–85, https://doi.org/10.5478/MSL.2018.9.3.81.
[56] B. Kunwar, K. Kawamura, One-year observations of carbonaceous and nitrogenous components and major ions in the aerosols from subtropical Okinawa Island, an outflow region of Asian dusts, Atmos. Chem. Phys. 14 (4) (2014) 1819–1836, https://doi.org/10.5194/acp-14-1819-2014.
[57] M. Koike, J. Ukita, J. Ström, P. Tunved, M. Shiobara, V. Vitale, A. Lupi, D. Baumgardner, C. Ritter, O. Hermansen, K. Yamada, C.A. Pedersen, Year-round *in situ* measurements of arctic low-level clouds: microphysical properties and their relationships with aerosols, J. Geophys. Res. Atmos. 124 (3) (2019) 1798–1822, https://doi.org/10.1029/2018JD029802.
[58] A. Lupi, M. Busetto, S. Becagli, F. Giardi, C. Lanconelli, M. Mazzola, R. Udisti, H.-C. Hansson, T. Henning, B. Petkov, J. Ström, R. Krejci, P. Tunved, A.P. Viola, V. Vitale, Multi-seasonal ultrafine aerosol particle number concentration measurements at the Gruvebadet observatory, Ny-Ålesund, Svalbard Islands, Rend. Lincei 27 (1) (2016) 59–71, https://doi.org/10.1007/s12210-016-0532-8.
[59] A.F. Stein, R.R. Draxler, G.D. Rolph, B.J.B. Stunder, M.D. Cohen, F. Ngan, NOAA's HYSPLIT atmospheric transport and dispersion modeling system, Bull. Am. Meterol. Soc. 96 (12) (2015) 2059–2077, https://doi.org/10.1175/BAMS-D-14-00110.1.
[60] Y.-K. Hsu, T.M. Holsen, P.K. Hopke, Comparison of hybrid receptor models to locate PCB sources in Chicago, Atmos. Environ. 37 (4) (2003) 545–562, https://doi.org/10.1016/S1352-2310(02)00886-5.
[61] K. Dimitriou, E. Remoundaki, E. Mantas, P. Kassomenos, Spatial distribution of source areas of $PM_{2.5}$ by concentration weighted trajectory (CWT) model applied in $PM_{2.5}$ concentration and composition data, Atmos. Environ. 116 (2015) 138–145, https://doi.org/10.1016/j.atmosenv.2015.06.021.
[62] C. Strong, I.G. Rigor, Arctic marginal ice zone trending wider in summer and narrower in winter, Geophys. Res. Lett. 40 (18) (2013) 4864–4868, https://doi.org/10.1002/grl.50928.
[63] R. Antony, A.M. Grannas, A.S. Willoughby, R.L. Sleighter, M. Thamban, P.G. Hatcher, Origin and sources of dissolved organic matter in snow on the East Antarctic ice sheet, Environ. Sci. Technol. 48 (11) (2014) 6151–6159, https://doi.org/10.1021/es405246a.
[64] B. Yang, K. Ljung, A.B. Nielsen, E. Fahlgren, D. Hammarlund, Impacts of long-term land use on terrestrial organic matter input to lakes based on lignin phenols in sediment records from a Swedish forest lake, Sci. Total Environ. 774 (2021) 145517, https://doi.org/10.1016/j.scitotenv.2021.145517.
[65] K. Eneroth, E. Kjellström, K. Holmén, A trajectory climatology for Svalbard: investigating how atmospheric flow patterns influence observed tracer concentrations, Phys. Chem. Earth 28 (28) (2003) 1191–1203, https://doi.org/10.1016/j.pce.2003.08.051.
[66] L. Schmeisser, J. Backman, J.A. Ogren, E. Andrews, E. Asmi, S. Starkweather, T. Uttal, M. Fiebig, S. Sharma, K. Eleftheriadis, S. Vratolis, M. Bergin, P. Tunved, A. Jefferson, Seasonality of aerosol optical properties in the Arctic, Atmos. Chem. Phys. 18 (16) (2018) 11599–11622, https://doi.org/10.5194/acp-18-11599-2018.
[67] E. Bednorz, D. Kaczmarek, P. Dudlik, Atmospheric conditions governing anomalies of the summer and winter cloudiness in Spitsbergen, Theor. Appl. Climatol. 123 (1) (2016) 1–10, https://doi.org/10.1007/s00704-014-1326-5.
[68] P.A. Matrai, L. Tranvik, C. Leck, J.C. Knulst, Are high Arctic surface microlayers a potential source of aerosol organic precursors? Mar. Chem. 108 (1) (2008) 109–122, https://doi.org/10.1016/j.marchem.2007.11.001.
[69] L.J. Beck, N. Sarnela, H. Junninen, C.J.M. Hoppe, O. Garmash, F. Bianchi, M. Riva, C. Rose, O. Peräkylä, D. Wimmer, O. Kausiala, T. Jokinen, L. Ahonen, J. Mikkilä, J. Hakala, X.-C. He, J. Kontkanen, K.K.E. Wolf, D. Cappelletti, M. Sipilä, Differing mechanisms of new particle formation at two Arctic sites, Geophys. Res. Lett. 48 (4) (2021) e2020GL091334, https://doi.org/10.1029/2020GL091334.
[70] P. Fu, K. Kawamura, J. Chen, M. Qin, L. Ren, Y. Sun, Z. Wang, L.A. Barrie, E. Tachibana, A. Ding, Y. Yamashita, Fluorescent water-soluble organic aerosols in the High Arctic atmosphere, Sci. Rep. 5 (1) (2015) 9845, https://doi.org/10.1038/srep09845.
[71] M.M. Haque, K. Kawamura, D.K. Deshmukh, B. Kunwar, Y. Kim, Biomass burning is an important source of organic aerosols in interior Alaska, J. Geophys. Res. Atmos. 126 (12) (2021) e2021JD034586, https://doi.org/10.1029/2021JD034586.
[72] R. Zangrando, E. Barbaro, P. Zennaro, S. Rossi, N.M. Kehrwald, J. Gabrieli, C. Barbante, A. Gambaro, Molecular markers of biomass burning in Arctic aerosols, Environ. Sci. Technol. 47 (15) (2013) 8565–8574, https://doi.org/10.1021/es400125r.
[73] A.M. Grannas, P.B. Shepson, T.R. Filley, Photochemistry and nature of organic matter in Arctic and Antarctic snow, Glob. Biogeochem. Cy. 18 (1) (2004), https://doi.org/10.1029/2003GB002133.
[74] M. Vecchiato, C. Barbante, E. Barbaro, F. Burgay, W.R.L. Cairns, A. Callegaro, D. Cappelletti, F. Dallo, M. D'Amico, M. Feltracco, J.-C. Gallet, A. Gambaro, C. Larose, N. Maffezzoli, M. Mazzola, I. Sartorato, F. Scoto, C. Turetta, M. Vardè, A. Spolaor, The seasonal change of PAHs in Svalbard surface snow, Environ. Pollut. 340 (2024) 122864, https://doi.org/10.1016/j.envpol.2023.122864.
[75] R. Benner, P. Louchouarn, R.M.W. Amon, Terrigenous dissolved organic matter in the Arctic Ocean and its transport to surface and deep waters of the North Atlantic, Glob. Biogeochem. Cy. 19 (2) (2005), https://doi.org/10.1029/2004GB002398.
[76] K. Kaiser, M. Canedo-Oropeza, R. McMahon, R.M.W. Amon, Origins and transformations of dissolved organic matter in large Arctic rivers, Sci. Rep. 7 (1) (2017) 13064, https://doi.org/10.1038/s41598-017-12729-1.
[77] P.J. Mann, R.G.M. Spencer, P.J. Hernes, J. Six, G.R. Aiken, S.E. Tank, J.W. McClelland, K.D. Butler, R.Y. Dyda, R.M. Holmes, Pan-Arctic trends in terrestrial dissolved organic matter from optical measurements, Front. Earth Sci. 4 (2016), https://doi.org/10.3389/feart.2016.00025.
[78] Y. Shen, R. Benner, L.L. Robbins, J.G. Wynn, Sources, distributions, and dynamics of dissolved organic matter in the Canada and Makarov Basins, Front. Mar. Sci. 3 (2016) 198, https://doi.org/10.3389/fmars.2016.00198.
[79] J.B. Pernov, D. Beddows, D.C. Thomas, M. Dall'Osto, R.M. Harrison, J. Schmale, H. Skov, A. Massling, Increased aerosol concentrations in the High Arctic attributable to changing atmospheric transport patterns, npj Clim. Atmos. Sci. 5 (1) (2022) 62, https://doi.org/10.1038/s41612-022-00286-y.
[80] S. Saallah, I.W. Lenggoro, Nanoparticles carrying biological molecules: recent advances and applications, KONA Powder Part. J. 35 (2018) 89–111, https://doi.org/10.14356/kona.2018015.
[81] B. Alberts, A. Johnson, J. Lewis, M. Raff, K. Roberts, P. Walter, Analyzing protein structure and function, in: Molecular Biology of the Cell, fourth ed., Garland Science, 2002.
[82] M. Österberg, M.H. Sipponen, B.D. Mattos, O.J. Rojas, Spherical lignin particles: a review on their sustainability and applications, Green Chem. 22 (9) (2020) 2712–2733, https://doi.org/10.1039/D0GC00096E.
[83] P. Widsten, S. Salo, T. Hakkarainen, T.L. Nguyen, M. Borrega, O. Fearon, Antimicrobial and flame-retardant coatings prepared from nano- and microparticles of unmodified and nitrogen-modified polyphenols, Polymers 15 (4) (2023) 992. https://www.mdpi.com/2073-4360/15/4/992.
[84] A. Holmgren, M. Norgren, L. Zhang, G. Henriksson, On the role of the monolignol γ-carbon functionality in lignin biopolymerization, Phytochem 70 (1) (2009) 147–155, https://doi.org/10.1016/j.phytochem.2008.10.014.
[85] C.H. Jung, Y.J. Yoon, H.J. Kang, Y. Gim, B.Y. Lee, J. Ström, R. Krejci, P. Tunved, The seasonal characteristics of cloud condensation nuclei (CCN) in the arctic

lower troposphere, Tellus B 70 (1) (2018) 1–13, https://doi.org/10.1080/16000889.2018.1513291.
[86] K.-T. Park, Y.J. Yoon, K. Lee, P. Tunved, R. Krejci, J. Ström, E. Jang, H.J. Kang, S. Jang, J. Park, B.Y. Lee, R. Traversi, S. Becagli, O. Hermansen, Dimethyl sulfide-induced increase in cloud condensation nuclei in the Arctic atmosphere, Glob. Biogeochem. Cy. 35 (7) (2021) e2021GB006969, https://doi.org/10.1029/2021GB006969.
[87] V.-M. Kerminen, X. Chen, V. Vakkari, T. Petäjä, M. Kulmala, F. Bianchi, Atmospheric new particle formation and growth: review of field observations, Environ. Res. Lett. 13 (10) (2018) 103003, https://doi.org/10.1088/1748-9326/aadf3c.
[88] M.D. Willis, J. Burkart, J.L. Thomas, F. Köllner, J. Schneider, H. Bozem, P.M. Hoor, A.A. Aliabadi, H. Schulz, A.B. Herber, W.R. Leaitch, J.P.D. Abbatt, Growth of nucleation mode particles in the summertime Arctic: a case study, Atmos. Chem. Phys. 16 (12) (2016) 7663–7679, https://doi.org/10.5194/acp-16-7663-2016.
[89] M. Rantanen, A.Y. Karpechko, A. Lipponen, K. Nordling, O. Hyvärinen, K. Ruosteenoja, T. Vihma, A. Laaksonen, The Arctic has warmed nearly four times faster than the globe since 1979, Commun. Earth Environ. 3 (1) (2022) 168, https://doi.org/10.1038/s43247-022-00498-3.
[90] R.Y.W. Chang, C. Leck, M. Graus, M. Müller, J. Paatero, J.F. Burkhart, A. Stohl, L.H. Orr, K. Hayden, S.M. Li, A. Hansel, M. Tjernström, W.R. Leaitch, J.P.D. Abbatt, Aerosol composition and sources in the central Arctic Ocean during ASCOS, Atmos. Chem. Phys. 11 (20) (2011) 10619–10636, https://doi.org/10.5194/acp-11-10619-2011.
[91] A.M.K. Hansen, K. Kristensen, Q.T. Nguyen, A. Zare, F. Cozzi, J.K. Nøjgaard, H. Skov, J. Brandt, J.H. Christensen, J. Ström, P. Tunved, R. Krejci, M. Glasius, Organosulfates and organic acids in Arctic aerosols: speciation, annual variation and concentration levels, Atmos. Chem. Phys. 14 (15) (2014) 7807–7823, https://doi.org/10.5194/acp-14-7807-2014.
[92] M. Ardyna, K.R. Arrigo, Phytoplankton dynamics in a changing Arctic Ocean, Nat. Clim. Change 10 (10) (2020) 892–903, https://doi.org/10.1038/s41558-020-0905-y.
[93] K.R. Arrigo, G. van Dijken, S. Pabi, Impact of a shrinking Arctic ice cover on marine primary production, Geophys. Res. Lett. 35 (19) (2008), https://doi.org/10.1029/2008GL035028.
[94] I.H. Myers-Smith, J.T. Kerby, G.K. Phoenix, J.W. Bjerke, H.E. Epstein, J.J. Assmann, C. John, L. Andreu-Hayles, S. Angers-Blondin, P.S.A. Beck, L.T. Berner, U.S. Bhatt, A.D. Bjorkman, D. Blok, A. Bryn, C.T. Christiansen, J.H.C. Cornelissen, A.M. Cunliffe, S.C. Elmendorf, S. Wipf, Complexity revealed in the greening of the Arctic, Nat. Clim. Change 10 (2) (2020) 106–117, https://doi.org/10.1038/s41558-019-0688-1.
[95] J. Terhaar, R. Lauerwald, P. Regnier, N. Gruber, L. Bopp, Around one third of current Arctic Ocean primary production sustained by rivers and coastal erosion, Nat. Commun. 12 (1) (2021) 169, https://doi.org/10.1038/s41467-020-20470-z.
[96] I.S. Cabral, I.R. Young, A. Toffoli, Long-term and seasonal variability of wind and wave extremes in the Arctic Ocean, Front. Mar. Sci. 9 (2022) 802022, https://doi.org/10.3389/fmars.2022.802022.
[97] D. Feng, C.J. Gleason, P. Lin, X. Yang, M. Pan, Y. Ishitsuka, Recent changes to Arctic river discharge, Nat. Commun. 12 (1) (2021) 6917, https://doi.org/10.1038/s41467-021-27228-1.
[98] D. Cappelletti, Ž. Ežerinskis, J. Šapolaitė, L. Bučinskas, B. Luks, A. Nawrot, C. Larose, P. Tuccella, J.C. Gallet, S. Crocchianti, F. Bruschi, B. Moroni, A. Spolaor, Long-range transport and deposition on the Arctic snowpack of nuclear contaminated particulate matter, J. Hazard Mater. 452 (2023) 131317, https://doi.org/10.1016/j.jhazmat.2023.131317.
[99] L. Dada, H. Angot, I. Beck, A. Baccarini, L.L.J. Quéléver, M. Boyer, T. Laurila, Z. Brasseur, G. Jozef, G. de Boer, M.D. Shupe, S. Henning, S. Bucci, M. Dütsch, A. Stohl, T. Petäjä, K.R. Daellenbach, T. Jokinen, J. Schmale, A central arctic extreme aerosol event triggered by a warm air-mass intrusion, Nat. Commun. 13 (1) (2022) 5290, https://doi.org/10.1038/s41467-022-32872-2.